Monografías de la Real Academia de Ciencias de Zaragoza. **22:** 75–82, (2003).

The dynamics of Kepler equation

V. Lanchares[1] and I. L. Pérez Barrón[2]

(1) Dept. Matemáticas y Computación

(2) Dept. Ingeniería Eléctrica

Universidad de La Rioja, 26004 Logroño, Spain. *

Abstract

It is well known that Kepler's equation can be solved by means of an iterative method defined, in a natural way, from the equation itself. This method yields to the unique solution if the eccentricity is in the range of the elliptic orbits. However, if we allow the eccentricity to take values greater than one or even in the complex plane, we discover a rich dynamics where period doubling bifurcations cascades are found, as well as fractal structures.

1 Introduction

May be Kepler's equation is the most studied nonlinear equation. In fact, a large number of papers are devoted to its solution in numerical or analytical form. Moulton [6] referred 123 papers on Kepler's equation in January 1900, and the list was incomplete. Nowadays, papers on Kepler's equation and its solution are still of scientific interest (see e.g. [7, 8]) and it shall be in the future. Thus, it is not infrequent to find Kepler's equation in the text books as an example to test different numerical methods. In this way, we found the following heading in a sheet of problems on numerical solutions of nonlinear equations

> *Use Newton's method to solve the Kepler's equation:* $E - e\sin E = M$*, for different values of* M *and* e *and different starting points.*

It is surprising that no restriction on the values of the eccentricity is considered. Indeed, from the point of view of Celestial Mechanics, Kepler's equation has no sense for $e \notin [0, 1)$. Nevertheless, as it is said in [1], the equation can be presented as a purely algebraic equation without any reference to an ellipse or an orbit. From this perspective, we are interested on the algebraic equation and the iterative processes to solve it from the point

*vlancha@dmc.unirioja.es, ivan.luis.perez@die.unirioja.es

of view of discrete dynamical systems. In particular, we will focus on the iterative process defined by the equation itself

$$E_{n+1} = M + e \sin E_n. \tag{1}$$

Let the function $F(x)$ defined as

$$F(x) = M + e \sin x. \tag{2}$$

Solving Kepler's equation is equivalent to find the fixed points of $F(x)$.

It is well known that Kepler's equation has a unique real root in the interval $[n\pi, (n+1)\pi]$ for $M \in [n\pi, (n+1)\pi]$ and $0 \leq e < 1$ [2]. Even more, the solution is unique for $-1 < e < 1$. It is an attracting solution if the absolute value of the first derivative

$$DF(x) = e \cos x, \tag{3}$$

is less than one. This is the case when $|e| < 1$. Thus, in the elliptic case the unique solution of the Kepler's equation is attractive and, moreover, the basin of attraction extends to $\pm\infty$ (any initial guess will converge to the solution). However, when the eccentricity is out of the range $|e| < 1$ different behavior is expected.

The function $F(x)$ can be considered as a shifted version of the sine map

$$G(x) = a \sin x, \tag{4}$$

studied by Feigenbaum in his celebrated work about the universal behavior in nonlinear systems [3]. There, it is shown that the mapping (4) behaves as the logistic map ($L(x) = \kappa x(1-x)$) as the parameter a ranges from 0 to π. Even more, this behavior is universal for the class of unimodal maps with negative Schwarzian derivative [5], that is defined, for a map ϕ, as

$$S_\phi = \frac{D^3\phi}{D\phi} - \frac{3}{2}\left(\frac{D^2\phi}{D\phi}\right)^2. \tag{5}$$

For the case of the Kepler map (2) we obtain

$$S_F = -1 - \frac{3}{2}\tan^2 x,$$

that is always negative it does not matter the values of the mean anomaly and the eccentricity.

Despite the dynamics of Kepler's equation is, to a certain extent, predictable, some interesting questions deserve a further insight: the influence of the shift produced by M in the pure sine map (4) and the behavior when the eccentricity is complex.

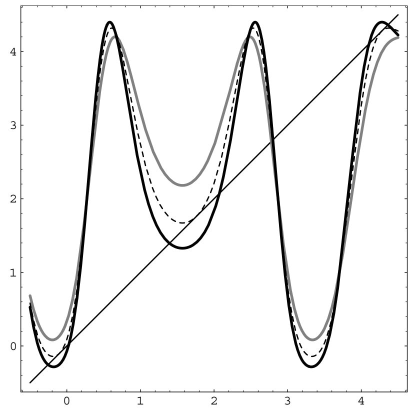

Figure 1: Born of a period three cycle for $M = 2$ as a consequence of a tangent bifurcation. Solid gray line is for $e = 2.2$, before the bifurcation. The dashed curve is for $e = 2.31922$, the bifurcation value. The black solid line is for $e = 2.4$, after the bifurcation. Six new period 3 points have appeared, arranged as two cycles, each of period 3, one stable and one unstable.

2 Bifurcations for real eccentricity

When $|e| \geq 1$ the absolute value of the derivative of $F(x)$ can exceed one and two kind of bifurcations are possible (see [4] pgs. 22–24)

(a) A period doubling (pitchfork) bifurcation if $F'(x) = -1$ at a fixed point.

(b) A tangent bifurcation if $F'(x) = 1$ at a fixed point.

The first one implies the loss of the attractive property of the fixed point while an attractive period two orbit appears. The second one implies the appearance of new fixed points and the lost of the attractive property of the fixed point. These two basic kinds of bifurcation processes can be extended to the k-iterate of the function $F(x)$ whose fixed points are cycles of period k.

It is worth to note that cycles of odd period only appear as a consequence of a tangent bifurcation and they do it in pairs (one stable, one unstable) as the graph of $F^k(x)$ moves to intercept the line $L(x) = x$ (see Figure 1).

If we consider the case $M = 0$, the first bifurcation takes place for $e = 1$. It is a tangent bifurcation and, as the value of e increases, a cascade of period doubling bifurcations is observed until a critical value of e is reached. If e continues increasing, cycles of odd period appear, the last one to do it the period three cycle (see Figure 2.a). A similar situation is observed for $M \neq 0$, but now, there is not a tangent bifurcation and the first period doubling bifurcation takes place for smaller values of the eccentricity, as it is shown in Figure 2.b. The extreme case is $M = \pi$ for which the first period doubling

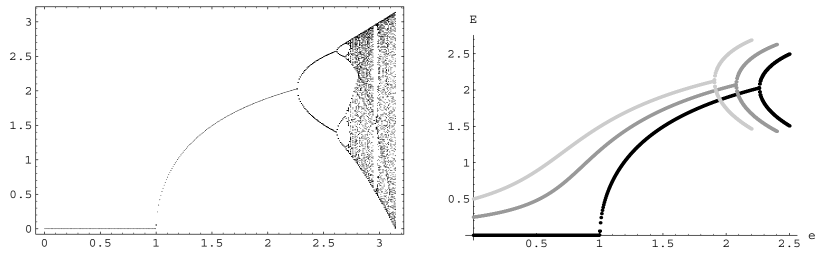

(a) (b)

Figure 2: (a) Cascade of period doubling bifurcation for the pure sine map $F(x) = e\sin x$. (b) The displacement of the first period doubling bifurcation as M increases. The curves stand for the values $M = 0$ in black, $M = 0.25$ in dark gray and $M = 0.5$.

bifurcation appears just at $e = 1$. Beyond $M = \pi$ the situation reverses and the first pitchfork bifurcation takes place for bigger values of e, in a symmetric way.

Proposition 1. *Let be $0 \le \alpha \le \pi$ and let (e_α, E_α) be the values of e and E at the first pitchfork bifurcation for $M = \pi - \alpha$, then $(e_\alpha, 2\pi - E_\alpha)$ are the values of e and E at the first pitchfork bifurcation for $M = \pi + \alpha$.*

Note that (e_α, E_α) solve the nonlinear system

$$\begin{aligned} &\pi - \alpha + e_\alpha \sin E_\alpha = E_\alpha, \\ &e_\alpha \cos E_\alpha = -1. \end{aligned} \tag{6}$$

The second equation is invariant if E_α is replaced by $2\pi - E_\alpha$. On the other hand, if π is added to the right and left hand members of the first equation we obtain, after arrangement,

$$\pi + \alpha - e_\alpha \sin E_\alpha = 2\pi - E_\alpha. \tag{7}$$

Taking into account that $\sin E_\alpha = -\sin(2\pi - E_\alpha)$ we finally arrive to

$$\pi + \alpha + e_\alpha \sin(2\pi - E_\alpha) = 2\pi - E_\alpha. \tag{8}$$

Thus, $(e_\alpha, 2\pi - E_\alpha)$ is a solution of the system (6) for $M = \pi + \alpha$ and then they are the values at the first pitchfork bifurcation. ■

A nice graphical description of both the symmetry and the displacement of the cascade of period doubling bifurcations, as M is tuned, may be obtained by means of a density plot of the k-iterate of the Kepler map for an initial starting point, we choose $E_0 = 0$. At the beginning, all the points in the plane (M, e) are the same color. As the function F is nested, the color of a point changes according to the value of $F^k(0)$. For the very first iterations, colors are distributed in a smooth way, so that small changes in the election of the pair (M, e) turns in small changes in the value of $F^k(0)$. However, if we iterate the function F a bit more, we observe color mixed areas whereas smooth regions of uniform

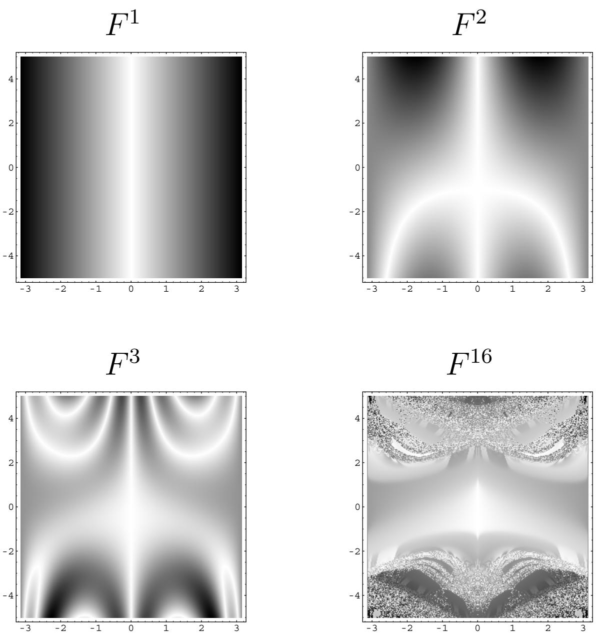

Figure 3: The iteration of F for $E_0 = 0$ in the plane (M, e). It can be viewed as the contours of the function $z = F^k(M, e; 0)$.

color are confined, in the most part, to the band $-1 < e < 1$ as it is shown in Figure 3. The mixing process is a direct consequence of the shift in the cascade of bifurcations produced by the variation of M. Worth noting is the symmetry respect to the line $M = \pi$, as it was pointed out in proposition 1. However, there is not symmetry respect to the line $e = 0$ (except for the first iteration) even in the case of the pure sine map ($M = 0$).

As much the map F is nested, the plots never reach a fixed image, nor a cyclic loop of images, unless the range of the eccentricity goes down the smallest accumulation point of period doubling of period 2^n. Nevertheless, even in such case, color mixed areas are found as a consequence of the shift produced by the variation of M.

3 Complex eccentricity

The Kepler map F can be extended to a complex map if we consider the parameters and the variable to be complex. In this way, we have the family of biparametric complex maps

$$F(M, e; z) = M + e \sin z, \qquad e, M, z \in \mathbb{C}. \tag{9}$$

It is clear that the sequence generated by iteration of the function F from a real starting point is bounded if M and e are real too. However, this is not the case for the complex map. In this way, it is enough that one of M, e, z_0 be complex to produce an unbounded sequence.

Taking this into account, we can generate a family of fractal sets defined in a similar way as it is the well known Mandelbrot set:

$$\mathcal{K}(M; z_0) = \{e \in \mathbb{C} \,|\, \{F^n(M, e; z_0)\}_{n\in\mathbb{N}} \text{ bounded}\}\,. \tag{10}$$

We also define the family of Julia sets associated to each pair (M, e)

$$\mathcal{J}(M, e) = \{z \in \mathbb{C} \,|\, \{F^n(M, e; z)\}_{n\in\mathbb{N}} \text{ bounded}\}\,. \tag{11}$$

Some properties of these sets are derived from the fact that the map (9) is symmetric respect to conjugation. Indeed, taking into account that $\sin \bar{z} = \overline{\sin z}$, we get

$$\overline{F(M, e; z)} = F(\bar{M}, \bar{e}; \bar{z}). \tag{12}$$

As a consequence, the set $\mathcal{K}(M; z_0)$ is symmetric respect to the real axis if both M and z_0 are real. In a similar way, $\mathcal{J}(M, e)$ is also symmetric respect to the real axis if both M and e are real.

In the case of the pure sine map, we have two additional symmetries

$$F^n(0, e : z) = (-1)^n F^n(0, -e; z), \qquad F^n(0, e; z) = -F^n(0, e; -z). \tag{13}$$

Then, the sets $\mathcal{K}(0; z_0)$ and $\mathcal{J}(0, e)$ are symmetric respect to the origin.

Finally, as $F(M, e; z) = F(M, e; z + 2k\pi)$, $k \in \mathbb{Z}$, the Julia set $\mathcal{J}(M, e)$ is, to a certain extent, periodic and it spread infinitely along the real axis. All these properties can be observed in Figure 4, where some fractal and Julia sets are shown.

4 Final remarks

1. It has be shown that Kepler's equation gives rise to an interesting dynamics if it is considered as a simple algebraic equation. Here, only one of the iterative processes to solve it has been studied. However, how is the dynamics if different iterative processes are considered? what happens if they are taken as circle maps $(\text{mod}\, 2\pi)$?.

2. The fractal sets $\mathcal{K}(M; z_0)$, defined in section 3, are clearly unbounded if $M, z_0 \in \mathbb{R}$, because they contain the real axis. However, it seems (see Figure 4) that they are confined to a band in the imaginary axis. Is this the case? and, what happens for $\mathcal{K}(M; z_0)$ if M or z_0 are not real? are these sets bounded or unbounded?

3. A similar question stands for Julia sets. Are they confined to a band in the imaginary axis?.

These questions and some other more make Kepler's equation attractive from a different point of view.

Acknowledgements

Support came in part from Universidad de La Rioja (Project API-99/B18) and from the Spanish Ministry of Education and Science (Project PB98-1576)

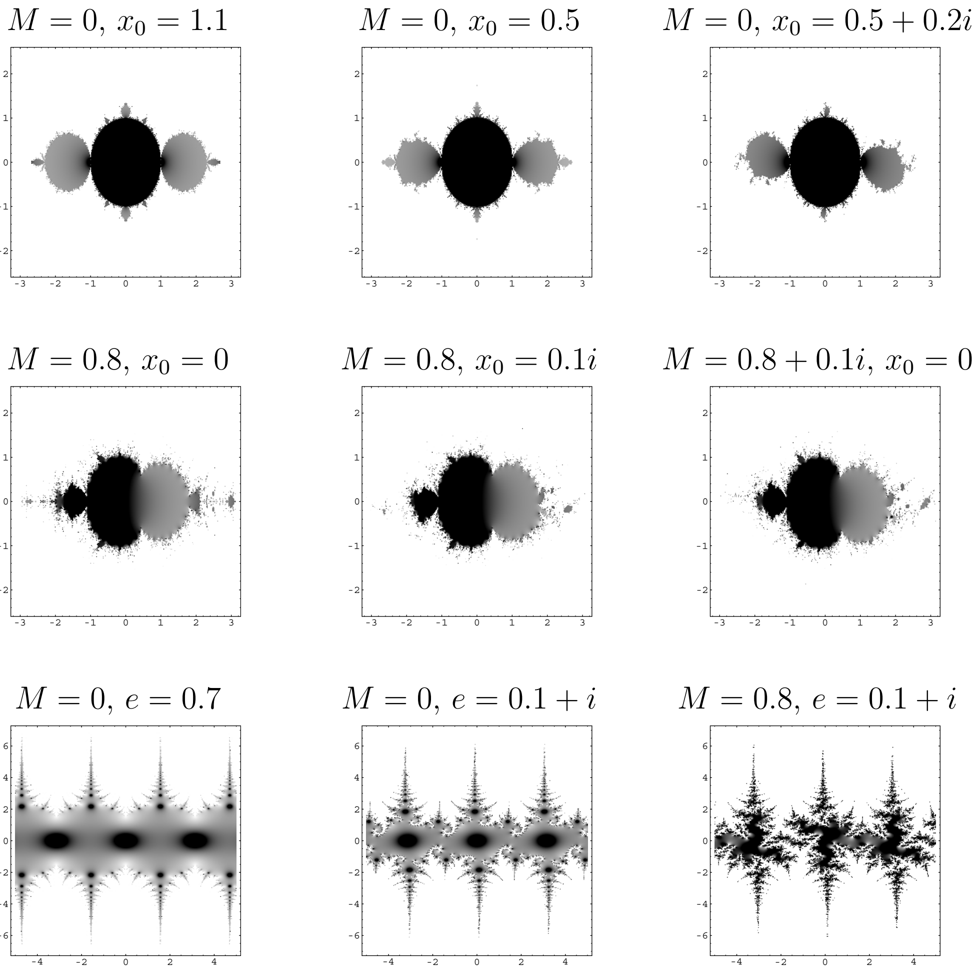

Figure 4: Different fractal and Julia sets for the Kepler complex map. The role of the symmetries, as the parameters change, is clearly visible.

References

[1] Charles, E. D. and Tatum, J. B.: 1998, 'The Convergence of the Newton-Raphson Iteration with Kepler's Equation', *Celestial Mechanics and Dynamical Astronomy*, **69**, 357–372.

[2] Danby, J. M. A.: 1988, *Fundamentals of Celestial Mechanics*, 2nd. edition. Willmann-Bell, Inc. Richmond.

[3] Feigenbaum, M. J.: 1983. 'Universal behavior in nonlinear systems', *Physica D*, **7**, 16–39.

[4] Hsu, C. S.: 1987, *Cell-to-Cell Mapping. A Method of Global Analysis for Nonlinear Systems*, Springer-Verlag. New York.

[5] Lyubich, M.: 2000 'The quadratic family as a qualitatively solvable model of chaos', *Notices of the American Mathematical Society*, **47**, 1042–1052.

[6] Moulton, F.R.: 1970, *An Introduction to Celestial Mechanics*, 2nd. revised edition. Dover. New York.

[7] Palacios, M.: 2002, 'Kepler equation and accelerated Newton method', *Journal of Computational and Applied Mathematics* **138**, 335–346.

[8] Stumpf, L.: 1999, 'Chaotic Behavior in the Newton Iterative Function Associated with Kepler's Equation', *Celestial Mechanics and Dynamical Astronomy*, **74**, 95–109.